Toroidal Condensates of Semiflexible Polymers in Poor Solvents: Adsorption, Stretching, and Compression

G. G. Pereira*† and D. R. M. Williams*

*Department of Applied Mathematics, Research School of Physical Sciences and Engineering, Australian National University, Canberra, Australian Capital Territory 0200, and †School of Chemistry, University of Sydney, New South Wales 2006, Australia

ABSTRACT When a semiflexible polymer chain is placed in a poor solvent, or in the presence of condensing agents, a toroidal condensate can result. In typical experiments, these condensates are adsorbed to surfaces. Here we examine the changes that can occur when a toroid is adsorbed. We then examine the behavior of a toroid when stretched and identify two regimes: a weak stretching regime where the toroid deforms from a circle to an ellipse, and a strong stretching regime where a tether is pulled from the toroid. In the weak stretching regime, the force increases linearly with separation whereas in the strong stretching regime, the applied force is a constant. We then look at the case of a toroid compressed in the plane of the toroid. In this case the form of the force law depends on how strongly the toroid wets the surfaces. In general, an inverse square force law is found.

INTRODUCTION

Unlike the case of semiflexible biopolymers, the equilibrium behavior of a fully flexible polymer in a poor solvent has been well understood for some time. The favorable monomer–monomer contacts drive the chain to minimize contact with the solvent. It thus forms a spherical globule because the sphere minimizes the polymer–solvent surface area at fixed volume. The globule is packed densely with polymer, and, in the simplest case where we are not very close to the theta point, all of the solvent is expelled from the globule. Thus, for fully flexible chains, we have a very simple scenario, a spherical ball of polymer. However, many polymers have significant bending rigidity, which implies a large free energy penalty for bending. These chains include a large number of biopolymers such as DNA and actin.

One of the areas of interest into these biological molecules stem from the insertion of genes into cells (Hansma et al., 1998; Phillips, 1995; Perales, 1994; Duguid, 1998). This is now of significant importance in medical research. Although up to now the most popular form of delivery has been virial-mediated gene delivery, questions of safety (Marshall, 1995) of this method has prompted research into receptor-based systems, where one condenses the DNA before it is put inside the cell. To image these molecules, various scanning probe microscopic techniques have been used. Of the many such techniques, atomic force microscopy (AFM) is becoming more and more widely used. For a full and recent review of this field, the reader is referred to the review article by Hansma and Pietrasanta (1998). Briefly, the AFM tip is used as a sensitive force sensor. The tip moves back and forth over the sample, sensing changes in characteristics of the surface, i.e., height. The tip may also oscillate up and down as it moves across the surface, mapping out the surface features (Hansma, 1999).

As mentioned above, the bending rigidity of biopolymer chains (such as DNA and actin) implies that a sphere is often not the most favorable morphology in a poor solvent, because a sphere implies a region of tight bend. It has been known for some time that semiflexible chains form toroids (Bloomfield, 1997, 1991; Fang et al., 1999; Fang and Hoh, 1998; Feng and Hoh, 1998; Hud et al., 1995; Odijk, 1996; Vasilevskaya et al., 1997; Yoshikawa et al., 1996). This is a reasonable compromise between the tendency to decrease surface area, and the need to have as little bend as possible. Toroidal condensates can form in poor solvents, although, experimentally, the usual procedure is to place some DNA in a good solvent and use a condensing agent (effectively a glue), which binds sections of the chains together. It has been realized by previous authors that the two problems (poor solvent and glue) are almost identical. In both cases, chain–chain contacts are favored. In some experiments, where the concentration of condensing agent is small, the two problems differ, but we will not consider this case here.

Although there is still some controversy surrounding the exact reason for the formation of toroids, there is one fairly simple model (Odijk, 1996; Grosberg, 1979; Ubbink and Odijk, 1995; Park et al., 1998; Bright and Williams, 1999) that accounts for most of the properties of toroids and gives a simple prediction for their size. This model has two terms in the free energy: a bending term and a surface term. These, together with the fact that the toroid is densely packed with polymer, are enough to calculate the major and minor radii of the toroid. The calculations produced thus far apply to isolated toroids in bulk solution.

However, in many cases, toroidal condensates are adsorbed to surfaces. This is true, for instance, in all cases

Received for publication 1 September 1999 and in final form 15 June 2000.

Dr. Pereira's present address is Cavendish Laboratory, University of Cambridge, Madingley Rd., Cambridge CB3 0HE, U.K.

Address reprint requests to Gerald G. Pereira, Cambridge University, Cavendish Laboratory TCM, Madingley Rd., Cambridge CB3 0HE, U.K. Tel.: +44-1223-337360; Fax: +44-1223-337356; E-mail: ggp21@phy.cam.ac.uk.

0006-3495/01/01/161/08 $2.00

where toroids have been imaged, either by AFM or electron microscopy. This is required for good imaging of the molecules (Golan et al., 1999; Argaman et al., 1997; Guthold et al., 1999; Hansma and Laney, 1996; Hansma et al., 1995; Radmacher et al., 1994). However, when the molecule becomes bound to the surface, it is natural and important to ask whether it is bound loosely enough for normal biological activity to occur. In this paper, we investigate a few important aspects of this. It is well known that, for fully flexible polymers, the chain conformation is drastically changed by adsorption to a surface. For toroidal condensates we might expect some changes upon adsorption. Indeed we will show here that there can be large changes in toroidal size and morphology upon adsorption. Furthermore, as discussed above, when, as the AFM tip maps out the surface of an object, e.g., biopolymer, it does so by tapping the tip softly across the surface. That is, the biopolymer can be crushed or stretched by the AFM tip. Thus, we are naturally led to the general subject of polymer deformation, in particular stretching and compression of the condensates. These are the second and third topics discussed in this paper. Our results will have important applications to these types of AFM experiments, where biological molecules are imaged.

TOROIDS IN BULK SOLUTION

For comparison with the adsorbed toroid case, it is instructive to consider the toroid conformation in bulk first. We will assume that thermodynamic equilibrium has been reached, so that we need to calculate the free energy of each possible conformation, and minimize this free energy over any free parameters. For a semiflexible chain in a poor solvent, there are two natural conformations: the rod and the toroid. The rod conformation, ignoring thermal fluctuations, has the free energy $F_{\text{rod}} = 4Lb\gamma_{\text{solv,poly}}$. Here, L is the length of the chain, and $\gamma_{\text{solv,poly}}$ is the interfacial tension between solvent and polymer. Here we assume that the monomers making up the chain are cubes of side b, hence the 4 in the free energy. It is convenient to make this energy dimensionless by defining $\sigma \equiv \gamma_{\text{solv,poly}} b^2/k_{\text{B}}T$ and $\mathcal{L} \equiv L/b$ so that the free energy becomes $F_{\text{rod}}/k_{\text{B}}T = 4\mathcal{L}\sigma$. The free energy of the toroid is made up of two terms—an interfacial energy term, as for the rod, and a bending energy term. The bending energy is given by

$$F_{\text{bend}} = \frac{1}{2} P k_{\text{B}} T \int_0^{\text{L}} c^2(s)\, \text{d}s, \tag{1}$$

where $c(s)$ is the local curvature of the chain. Here P is the persistence length: the larger the value of P the more rigid the chain. From now on we make the assumption of a thin toroid. By thin we mean that the minor radius of the toroid is much smaller than the major radius, i.e., the toroid has a large hole compared to its thickness (Fig. 1). This considerably simplies the calculation of the bending energy because all the chains have the same curvature $c = 1/R$ where R is the major radius of the toroid. The bending free energy is then $F_{\text{bend}} = \frac{1}{2} P k_{\text{B}} T L R^{-2}$. The surface area of the toroid is $2\pi R \times 2\pi r$ where r is the minor radius of the toroid. This gives an interfacial energy of $4\pi^2 R r \gamma_{\text{solv,poly}}$. The toroidal volume is $2\pi R \times \pi r^2$, which must equal the volume of the polymer, $b^2 L$. This allows us to eliminate r and obtain a dimensionless free energy of the toroid as

$$\frac{F}{k_{\text{B}}T} = \frac{1}{2}\mathcal{L}\mathcal{P}\mathcal{R}^{-2} + 2\pi\sqrt{2}\sigma(\mathcal{L}\mathcal{R})^{1/2}, \tag{2}$$

where $\mathcal{P} \equiv P/b$ and $\mathcal{R} = R/b$. There exists an optimum radius for the toroid obtained by minimizing F_{toroid} with respect to $\mathcal{R}$. Doing this, one finds that the optimal radius is

$$\mathcal{R}_{\text{eq}} = \left(\frac{\mathcal{L}\mathcal{P}^2}{2\pi^2\sigma^2}\right)^{1/5}. \tag{3}$$

The corresponding minimum free energy of the toroid is

$$\frac{\mathcal{F}_{\text{eq}}}{k_{\text{B}}T} = \left(\frac{3125}{8}\pi^4\sigma^4\mathcal{L}^3\mathcal{P}\right)^{1/5}. \tag{4}$$

By comparing the rod free energy to the toroid free energy, we can show that a transition of rods to toroids occurs when $\mathcal{L} = 6.096\sqrt{\mathcal{P}/\sigma}$.

In fact, near the transition point, our approximation of a complete toroid breaks down. A better model near the transition consists of a partial loop or "proto-toroid." In this case, a similar analysis (Bright and Williams, 1999) gives a critical length for the transition from rod to loop of $\mathcal{L} = 8.16\sqrt{\mathcal{P}/\sigma}$, i.e., the same result but with a slightly different prefactor. In any case, the prediction is that for small chain lengths we obtain rods, whereas for larger chain lengths toroids are produced.

ADSORBED TOROIDS

In the previous section, a simple argument was presented to determine when toroids formed in bulk solution. Here we

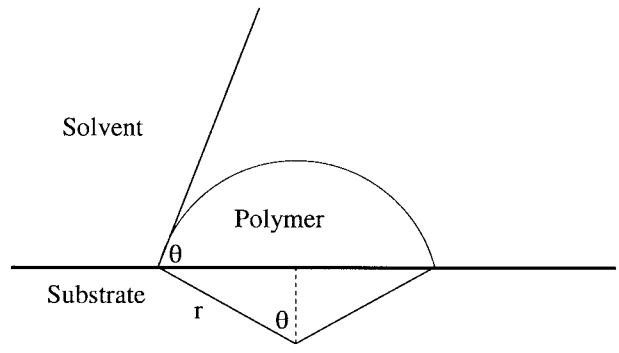

FIGURE 1 Cross section of an adsorbed toroid.

examine what happens when the toroid is absorbed to a surface, as often happens experimentally. Once again we consider the situation where the toroid radius is large compared to the cross-sectional radius. This is a good approximation for chains close to the transition line because there the number of loops is small and so the toroid radius is large. Only for very poor solvents does the cross-sectional radius become comparable to the toroid radius.

Consider Fig. 1, which is a schematic of our model. The cross section of the toroid is part of a circle of radius r. First consider determining the interfacial energy for this model. It is made of substrate–polymer contribution and a solvent–polymer contribution. The contact angle of the toroidal polymer droplet, θ, is given simply by Young's Equation,

$$\cos\theta = \frac{\sigma_{\mathrm{solv,subs}} - \sigma_{\mathrm{subs,poly}}}{\sigma}, \tag{5}$$

where $\sigma_{\mathrm{solv,subs}}$ and $\sigma_{\mathrm{poly,subs}}$ are the (dimensionless) solvent–substrate and substrate–polymer interfacial tensions, respectively. Now the cross-sectional area is $A = \theta r^2 - r^2 \cos\theta \sin\theta$, where r is the radius of the cross-section. If R is the toroid radius, from volume conservation we have

$$r = \sqrt{\frac{Lb^2}{2\pi R(\theta - \cos\theta \sin\theta)}}. \tag{6}$$

The interfacial energy now has two contributions, one due to the solvent–polymer interaction and the other due to the substrate–polymer interaction. These two terms can be determined using Fig. 1 and some elementary geometry, giving an interfacial energy contribution,

$$F_{\mathrm{int}} = 2\theta r 2\pi R\gamma_{\mathrm{solv,poly}} + 2r\sin\theta 2\pi R(\gamma_{\mathrm{subs,poly}} - \gamma_{\mathrm{solv,subs}}). \tag{7}$$

Using Eq. 6 for r and making the quantities dimensionless, we find

$$\frac{F_{\mathrm{int}}}{k_{\mathrm{B}}T} = 2\sqrt{2\pi}(\mathcal{R}\mathcal{L})^{1/2}\sqrt{\theta - \sin\theta\cos\theta}. \tag{8}$$

The bending energy of the toroid can be approximated by the same expression as we used for the three-dimensional (3D) case because we have $R \gg r$. Thus the free energy of the adsorbed toroid is

$$\frac{F}{k_{\mathrm{B}}T} = \frac{1}{2}\frac{\mathcal{P}\mathcal{L}}{\mathcal{R}^2} + 2\sqrt{2\pi}(\mathcal{R}\mathcal{L})^{1/2}\sqrt{\theta - \sin\theta\cos\theta}. \tag{9}$$

This expression is the same as the expression for the 3D toroid, with the modification that σ is changed to $\eta = \sigma\sqrt{(\theta - \sin\theta\cos\theta)/\pi}$. Under this substitution, we can find the optimal radius $\mathcal{R}$ of the toroid $\mathcal{R} = \mathcal{R}_{\mathrm{eq}}[\pi/(\theta - \sin\theta\cos\theta)]^{1/5}$ and free energy

$$\frac{F_{\mathrm{min}}}{k_{\mathrm{B}}T} = \left[\frac{3125}{8}\pi^2\sigma^4\mathcal{L}^3\mathcal{P}(\theta - \sin\theta\cos\theta)^2\right]^{1/5} = \frac{\mathcal{F}_{\mathrm{eq}}}{k_{\mathrm{B}}T}[(\theta - \sin\theta\cos\theta)/\pi)]^{2/5}. \tag{10}$$

Here $\mathcal{R}_{\mathrm{eq}}$ and $\mathcal{F}_{\mathrm{eq}}$ are the results for a toroid in bulk solution, i.e., Eqs. 3 and 4. Note in particular that, in the two limits of perfect wetting $\theta \to 0$ and nonwetting $\theta \to \pi$, we obtain

$$\begin{aligned} \mathcal{R} &= \mathcal{R}_{\mathrm{eq}}\left(\frac{3\pi}{2\theta^3}\right)^{1/5} && \theta \to 0 \\ \mathcal{R} &= \mathcal{R}_{\mathrm{eq}}\left[1 - \frac{2}{15\pi}(\theta - \pi)^3\right] && \theta \to \pi \end{aligned} \tag{11}$$

In general, adsorption leads to an increase in radius. For the particular case of $\theta = \pi/2$, the increase is 15%, whereas, for $\theta = 0.5$, the increase is more than 100%. In our calculation of the adsorbed toroid, we have adopted a continuum model of the chain packing. In actual fact, the chains have a finite width b, so that the thickness of the adsorbed toroid $r(1 - \cos\theta)$ must be at least b. This leads to an inequality for the continuum model to be valid:

$$\mathcal{L} > 2\pi\sqrt{\frac{\mathcal{P}}{\sigma}}\frac{\theta - \sin\theta\cos\theta}{(1 - \cos\theta)^{5/2}}. \tag{12}$$

When this inequality is violated, the toroid adopts a completely flat morphology, i.e., it is squashed onto the surface as a monolayer. We can readily calculate the free energy of this morphology, assuming many turns. It consists of only two terms, the usual bending term and a term associated with the area of the two side surfaces

$$\frac{F}{k_{\mathrm{B}}T} = \frac{1}{2}\frac{\mathcal{P}\mathcal{L}}{\mathcal{R}^2} + 4\pi\mathcal{R}\sigma. \tag{13}$$

Note that the top and bottom surfaces do not play a role because these are independent of $\mathcal{R}$. Minimizing over $\mathcal{R}$ yields $\mathcal{R} = (\mathcal{P}\mathcal{L}/4\pi\sigma)^{1/3}$. Note that, here, $\mathcal{R}$ has a stronger dependence upon length than is found for the partially adsorbed toroid or the toroid in bulk solution.

We conclude this section by noting one fairly obvious point. Surface energies should not strongly affect whether a prototoroid is formed, because this is a two-dimensional process. This means that, if a prototoroid is found on a surface, it is almost certainly to be found in bulk solution. However, adsorption can dramatically change the toroidal size and toroidal morphology.

STRETCHING

The subject of polymer deformation has a central position in polymer science. This is mainly because, in almost all cases

of interest, polymers are deformed by their environment. The case of an ordinary fully flexible polymer in a poor solvent has been discussed by Halperin and Zhulina (1991). They showed that, for weak deformations, an initially spherical globule deforms into an ellipsoid. At stronger deformations the polymer breaks up into a "ball and chain" or tadpole configuration, where most of the chain is confined to a ball while the remainder forms a long tail. This is effectively the Rayleigh–Plateau instability (Plateau, 1873; Rayleigh, 1879) for a polymer, i.e., a long cylinder of fluid is unstable to undulations because these reduce the surface energy. It is fairly clear that this kind of behavior should also occur for toroidal condensates. Here we examine this in detail, first looking at the case of a circular toroid deformed into an ellipse.

Consider deforming a semiflexible polymer in a poor solvent by stretching it so its ends are a distance X apart. Let us assume that, when stretched, the toroidal polymer becomes an ellipse, with equation

$$\frac{x^2}{\alpha^2} + \frac{y^2}{\beta^2} = 1, \tag{14}$$

or in parametric form

$$x = \alpha\cos(t), \quad y = \beta\sin(t) \quad \text{where} \quad 0 < t < 2\pi, \tag{15}$$

with semimajor axis $\alpha = X/2$ and semiminor axis β. Now we need to determine the Helmholtz free energy of the system F where $F = F_{\text{surf}} + F_{\text{bend}}$. Let us first determine the surface free energy of the toroid. It is given by the polymer–solvent surface tension times the area of the toroid. The latter is equal to the $2\pi rC$, where r is the minor radius of the toroid (assumed to have circular cross section) and C is the perimeter of the ellipse. C is given, to leading order in e, by $4\alpha E(e)$ where $E(e)$ is an elliptic function of the second kind (Abramowitz and Stegun, 1970), and $e \equiv \sqrt{1 - \beta^2/\alpha^2}$ is the eccentricity of the ellipse. We find then

$$F_{\text{surf}} = 8\gamma_{\text{solv,poly}}\pi r\alpha E(e). \tag{16}$$

Now, the radius of the cross-section can be determined from the volume restriction, i.e., $Lb^2 = \pi r^2 C$ so that $r = \sqrt{Lb^2/(4\pi\alpha E(e))}$, and the surface free energy is

$$F_{\text{surf}}/k_{\text{B}}T = 4\sigma\sqrt{a\pi E(e)\mathcal{L}}, \tag{17}$$

where $a \equiv \alpha/b$.

The bending energy is given by Eq. 1. The curvature at any point is $c(s) = \mathrm{d}\tau/\mathrm{d}s$, where τ is the angle made by the tangent to the ellipse with some fixed axis, and s is the arc length of the curve at that point. This is best calculated using the parametric form of the ellipse. If we call τ the angle made by the tangent to the ellipse with the negative y axis, then $\tan(\tau) = -\mathrm{d}x/\mathrm{d}y = (\alpha/\beta)\tan(t)$. The bending energy can be written as

$$F_{\text{bend}} = \frac{1}{2}Pk_{\text{B}}T\int_0^{\text{L}}\mathrm{d}s\left(\frac{\mathrm{d}\tau}{\mathrm{d}s}\right)^2 = 2Pk_{\text{B}}T(L/C)\int_0^{\pi/2}\mathrm{d}\tau\frac{\mathrm{d}\tau}{\mathrm{d}s}. \tag{18}$$

We now convert from τ to t so that $\mathrm{d}\tau = (\alpha/\beta)\mathrm{d}t\,\sec^2 t(1 + (\alpha/\beta)^2\tan^2 t)^{-1}$ and $\mathrm{d}s = \sqrt{\mathrm{d}x^2 + \mathrm{d}y^2} = \alpha\,\mathrm{d}t\sqrt{1 - e^2\cos^2 t}$. This gives a bending free energy

$$F_{\text{bend}} = \frac{1}{2}\frac{Pk_{\text{B}}TL(1 - e^2)J(e)}{\alpha^2 E(e)}, \tag{19}$$

where $J(e)$ is given by

$$J(e) = \int_0^{\pi/2}\mathrm{d}t\,\frac{1}{[1 - e^2\cos^2 t]^{5/2}}. \tag{20}$$

Thus the dimensionless bending energy becomes

$$\frac{F_{\text{bend}}}{k_{\text{B}}T} = \frac{\mathcal{P}\mathcal{L}(1 - e^2)J(e)}{2a^2E(e)}. \tag{21}$$

The Helmholtz free energy then becomes

$$\frac{F_{\text{ellipse}}}{k_{\text{B}}T} = 4\sigma\sqrt{a\pi E(e)\mathcal{L}} + \frac{\mathcal{P}\mathcal{L}(1 - e^2)J(e)}{2a^2E(e)}. \tag{22}$$

For a given extension (i.e., given a) we need to minimize this over the eccentricity e. Minimizing over e and assuming $e \ll 1$ yields

$$\frac{F_{\text{ellipse}}}{k_{\text{B}}T} \approx \frac{5}{2}\pi\sigma\sqrt{2\mathcal{L}\mathcal{R}_{\text{eq}}}\left[1 + \frac{9}{28}\mathcal{R}_{\text{eq}}^{-2}(a - \mathcal{R}_{\text{eq}})^2\right] = \frac{\mathcal{F}_{\text{eq}}}{k_{\text{B}}T}\left[1 + \frac{9}{28}\mathcal{R}_{\text{eq}}^{-2}(a - \mathcal{R}_{\text{eq}})^2\right] \tag{23}$$

where $\mathcal{R}_{\text{eq}}$ is the equilibrium radius of the circular toroid given earlier in Eq. 3. The optimum eccentricity at fixed a is

$$e_{\text{opt}} \approx \frac{\sqrt{70}}{7}\left(\frac{a}{\mathcal{R}_{\text{eq}}} - 1\right)^{1/2} + \frac{41}{392}\sqrt{70}\left(\frac{a}{\mathcal{R}_{\text{eq}}} - 1\right)^{3/2}. \tag{24}$$

The force, M, needed to stretch the toroid can be found by differentiating the free energy with respect to 2α. The dimensionless force $f = Mb/kT$ is $f \approx {}^{45}\!/_{56}\,\pi\sigma\sqrt{2\mathcal{R}_{\text{eq}}\mathcal{L}}\mathcal{R}_{\text{eq}}^{-2}(a - \mathcal{R}_{\text{eq}})$. This is, as we would expect, a force linear in the extension at weak extensions. This formula is also valid at weak compressions. The more typical case, where the toroid is compressed in the other plane, is discussed in the next section.

The calculation is valid provided the chain is not stretched too far. At larger displacements, the chain no longer forms an ellipse but forms a (lifebuoy + tether) or tadpole configuration (see Fig. 2), where the toroid is circular but sends out a tether that takes up most of the stretch. This structure, therefore, has a free energy that consists of (approximately) the undistorted toroid free energy plus an extra surface energy due to the tail being exposed to solvent.

The Helmholtz free energy of the tadpole configuration stretched apart a distance $X = xb$ is then

$$\frac{F_{\text{tad}}}{k_{\text{B}}T} = 4\sigma(x - \mathcal{R}_{\text{eq}}) + \frac{5}{2}\pi\sigma\sqrt{2\mathcal{L}\mathcal{R}_{\text{eq}}}. \qquad (25)$$

Here we have made two approximations. 1) The tether originates tangentially from the toroidal head. 2) The radius and free energy of the head are the same as in the undistorted case, i.e., we have neglected that some of the length of the chain is used in the tail. This assumption is probably very good all the time, because, if the tail is short it is obviously good, and if the tail is long the free energy is dominated by the tail and the head plays little part. Note that the force law for a tadpole configuration is a constant $f = 4\sigma$.

Under conditions of fixed extension, we need to find when the elliptical configuration changes to a tadpole configuration. This can be found by equating the two Helmholtz free energies (with $x = 2a$) to give an equation

$$4\sigma(x - \mathcal{R}_{\text{eq}}) - \frac{45}{56}\pi\sigma\sqrt{2\mathcal{L}\mathcal{R}_{\text{eq}}}\mathcal{R}_{\text{eq}}^{-2}\left(\frac{x}{2} - \mathcal{R}_{\text{eq}}\right)^2 = 0. \qquad (26)$$

Solving this in the approximation that $\mathcal{R}_{\text{eq}} \ll \mathcal{L}$ yields $x = 2\mathcal{R}_{\text{eq}}[1 + 1.06(\mathcal{R}_{\text{eq}}/\mathcal{L})^{1/4}]$. Note that, at the transition, this expansion would predict the eccentricity is $e \approx 1.2(\mathcal{R}_{\text{eq}}/\mathcal{L})^{1/8}$ so that we must have $\mathcal{R}_{\text{eq}}$ very much less than $\mathcal{L}$ so that our approximation of small eccentricity holds. In this limit, the ellipse becomes a tadpole rather rapidly, because, if $\mathcal{R}_{\text{eq}} \ll \mathcal{L}$, the critical value of x lies very close to $2\mathcal{R}_{\text{eq}}$.

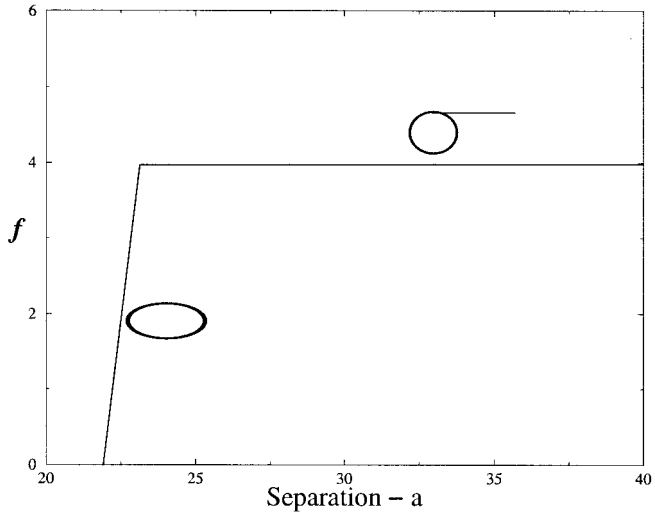

FIGURE 2 $f = Mb/k_{\text{B}}T$ versus separation a for stretching a chain between two points. The parameters used for this plot are $\mathcal{L} = 10^4$, $\mathcal{P} = 10^2$, $\sigma = 1$, and so we are in the toroidal regime with $\mathcal{R}_{\text{eq}} = 21.9$.

We have considered the case of stretching the polymer at a given separation. One may alternatively ask, for given force how does the polymer deform? Of course the two cases are quite similar. In the second case, one calculates the Gibbs energy of the system, which is $G/k_{\text{B}}T = F_{\text{bend}}/k_{\text{B}}T + F_{\text{surf}}/k_{\text{B}}T - 2f(a - \mathcal{R}_{\text{eq}})$, where F_{bend} and F_{surf} are as above, for the various configurations. The Gibbs energy is a function of two variables a and e^2. Minimizing numerically with respect to both of them, one obtains a force versus separation curve as in Fig. 2. Note the change in force law (linear to constant) at $f = 4$ corresponding to an elliptic-to-tadpole transition.

COMPRESSION

The next case we consider is compression of the toroidal polymer in a poor solvent. When the toroid is compressed between two flat parallel planes, there are two possible scenarios. First, the toroid could lie in a plane parallel to the confining planes, or, second, perpendicular to the planes. The second scenario is not likely to occur because any small perturbation will cause the toroid to tip over. Thus we analyze the first scenario here. When the toroid lies parallel to the planes there are two possible deformations of the toroid. These correspond to the toroid polymer droplet not wetting the substrate, as in Fig. 3 *A*, or where the droplet does wet the substrate, as in Fig. 3 *B*.

We initially discuss the case where the contact angle is equal to π. In this case, compression of the toroid between two surfaces leads to deformation of the cross section. For weak compressions, the cross section changes from a circle to an ellipse. Let the distance between the two plates be H and the major and minor axes of the ellipse be r_1 and r_2. We introduce dimensionless variables $\mathcal{H} \equiv H/b$, $\rho_1 = r_1/b$, and $\rho_2 = r_2/b$ and clearly, $\mathcal{H} = 2\rho_2$. The cross-sectional area of the ellipse is $\pi r_1 r_2$ and the volume of the toroid is $Lb^2 = 2\pi R(\pi r_1 r_2)$. This leads to the equation

$$\rho_1 = \mathcal{L}/(\pi^2\mathcal{H}\mathcal{R}). \qquad (27)$$

The surface area of the toroid is just $2\pi R$ times the perimeter of the ellipse $4r_1E(e)$ where the eccentricity is $e = \sqrt{1 - (r_2/r_1)^2} = \sqrt{1 - \pi^4\mathcal{R}^2\mathcal{H}^4/\mathcal{L}^2}$. The Helmholtz free energy is then

$$\frac{\mathcal{F}}{k_{\text{B}}T} = \frac{1}{2}\frac{\mathcal{P}\mathcal{L}}{\mathcal{R}^2} + \frac{8\mathcal{L}}{\pi\mathcal{H}}E(e)\sigma. \qquad (28)$$

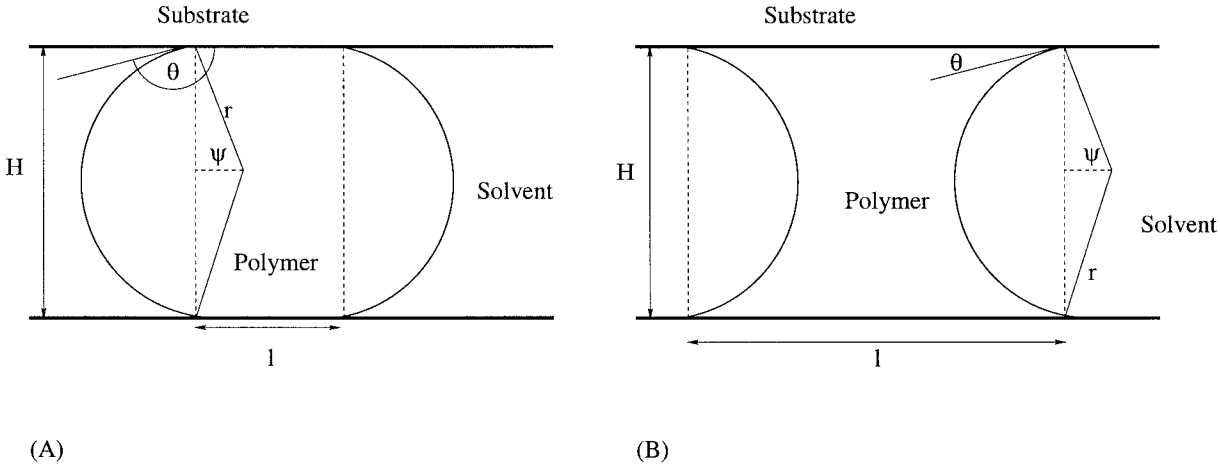

FIGURE 3 Conformation of toroidal polymer between confining plates for (*A*) the nonwetting case and (*B*) the wetting case.

This can also be written

$$\frac{\mathcal{F}}{k_B T} = \sigma \frac{\pi}{\sqrt{2}} \sqrt{\mathcal{L}\mathcal{R}_{eq}^5}\mathcal{R}^{-2} + 4\sigma\sqrt{2\mathcal{L}\mathcal{R}_{eq}}\epsilon^{-1}E(\sqrt{1-\epsilon^4\mathcal{R}^2\mathcal{R}_{eq}^{-2}}). \quad (29)$$

where $\epsilon \equiv H/(2r_{eq})$ is the ratio of the compressed thickness to the thickness under no compression.

Expanding the free energy about $\epsilon = 1$ and minimizing over R yields $\mathcal{R} = \mathcal{R}_{eq}[1 + {}^{16}\!/_{3}(1 - \epsilon)]$ and

$$\frac{\mathcal{F}}{k_B T} = \mathcal{F}_{eq}\left(1 + \frac{6}{13}(\epsilon - 1)^2\right). \quad (30)$$

This gives, as we would expect, a force that is linear in the compression.

For very strong compressions, where $\epsilon \to 0$, we can also expand the free energy and obtain $\mathcal{R} \approx \mathcal{R}_{eq}\epsilon^{-2}(4\exp(-1) - (\pi/256)\exp(3)\epsilon^5)$ and a free energy of

$$F/k_B T \approx 4\sigma\sqrt{\mathcal{L}\mathcal{R}_{eq}}[1 + 4\exp(-2)]\epsilon^{-2}. \quad (31)$$

This gives a force law that varies inversely as the cube of distance between the two surfaces.

Let us consider now what happens when $\theta < \pi$. In this case, when the toroid gets squashed, the cross section of the toroid consists of a flattened section with two caps (see Fig. 3). Once again we assume the toroidal radius R is much greater than the radius of a cross section r. In this case, the bending term can be approximated using the one radius of curvature R. When the droplet does not wet the substrate, the contact angle θ is greater than $\pi/2$. We must determine the cross-sectional area of the toroid, which is the sum of the rectangular part of dimensions l by H and the two sectors at each end. The area of the sector is $A_s = \psi r^2 - (1/2)rH\cos\psi$, where ψ is the half angle of the sector and r is the radius of the sector. Now $\psi = \theta - \pi/2$ and the radius of the sector is related to the contact angle and d by $\cos\theta = -H/(2r)$. Thus the total cross-sectional area of the droplet is $A_{XS} = lH + (H^2/2)\{(\theta - \pi/2)/\cos^2\theta + \tan\theta\}$. Using conservation of volume for the toroid, we can write l in terms of the toroid radius R and the plate separation H:

$$l = \frac{Lb^2}{2\pi RH} - \frac{H}{2}\left(\frac{\theta - \pi/2}{\cos^2\theta} + \tan\theta\right). \quad (32)$$

The polymer–substrate contact area is thus $4\pi Rl$ with l given above. To obtain the polymer–solvent contact area, we require to know the perimeter of the sectors at each end. This perimeter length is $2\psi r$. Substituting for ψ and R as before, we find that the polymer-solvent contact area is $4\pi RH(\pi/2 - \theta)/\cos\theta$. We get the same answers for the solvent–polymer area and surface–polymer area for the case $0 < \theta < \pi/2$.

The Helmholtz free energy for this configuration, after appropriately scaling all parameters, is

$$\frac{F_{toroid}}{k_B T} = \frac{4\pi\mathcal{R}\mathcal{H}(\pi/2 - \theta)}{\cos\theta}\sigma + \left[\frac{2\mathcal{L}}{\mathcal{H}} + 2\pi\mathcal{R}\mathcal{H}\left(\frac{\pi/2 - \theta}{\cos^2\theta} - \tan\theta\right)\right] \cdot (\sigma_{subs,poly} - \sigma_{subs,solv}) + \frac{\mathcal{P}\mathcal{L}}{2\mathcal{R}^2}. \quad (33)$$

This may be written in the simpler form,

$$\frac{F_{toroid}}{k_B T} = \kappa(\theta, \sigma)\mathcal{R}\mathcal{H} - \frac{2\mathcal{L}\sigma}{\mathcal{H}}\cos\theta + \frac{\mathcal{P}\mathcal{L}}{2\mathcal{R}^2}, \quad (34)$$

where $\kappa(\theta, \sigma) = \sigma\pi[\pi - 2\theta - \sin(2\theta)]/\cos\theta$. Note that κ is positive for $0 < \theta < \pi$. Minimizing this free energy at fixed separation leads to an optimal toroidal radius $\mathcal{R} = (\mathcal{P}\mathcal{L}/\mathcal{H}\kappa)^{1/3}$. The minimum free energy for the system is

then

$$\frac{F_{\text{toroid}}}{k_B T} = \frac{3(\mathcal{P}\mathcal{L}\kappa^2)^{1/3}\mathcal{H}^{2/3}}{2} - \frac{2\mathcal{L}}{\mathcal{H}}\cos\theta\sigma. \qquad (35)$$

Thus the force required to compress the chain is the derivative of this free energy with respect to $-\mathcal{H}$ (since the separation is decreasing) is

$$f = -2\mathcal{L}\cos\theta\sigma\mathcal{H}^{-2} - (\mathcal{P}\mathcal{L}\kappa^2)^{1/3}\mathcal{H}^{-1/3}. \qquad (36)$$

Note that the coefficient of $\mathcal{H}$ in the first term of the force law is much larger than the coefficient of $\mathcal{H}$ in the second term, i.e., $\mathcal{L}$ compared with $(\mathcal{L}\mathcal{P})^{1/3}$. Thus the first term is the dominant term. In the nonwetting case, $(\theta > \pi/2)\cos\theta$ is negative, so we require a positive force, proportional to $\mathcal{H}^{-2}$, to compress the polymer. For $\theta \leq \pi/2$, a negative force is required, i.e., a force in the opposite direction. This can be attributed to two factors. In the wetting case ($\theta < \pi/2$) because the substrate prefers the polymer to the solvent, the polymer preferentially spreads on the substrate. This situation is analogous to a wetting fluid imbibing through a porous medium or up a narrow capillary. Second, after $\theta \leq \pi/2$, both $\mathcal{H}$-dependent terms in the free energy are minimized by the smallest possible $\mathcal{H}$, i.e., $\mathcal{H} = 1$. The combination of these two factors implies that a force is required to prevent the plates from collapsing together. The difference in scaling laws for $\theta = \pi$ ($f \propto H^{-3}$) and $\theta < \pi$ ($f \propto H^{-2}$) can be attributed to the extra substrate–polymer contact term for the later case.

Note that the magnitude of the forces required to compress these chains is much larger than that required to stretch them. For example, these forces are of the order $\mathcal{L}\cos\theta\sigma$, whereas, in the stretching case, the maximum force is 4σ. The main reasons for this are that, when the polymer gets compressed, the resulting cross-sectional conformation greatly increases the overall interfacial contact area. For example, if the contact angle is $\pi/2$ (i.e., a square cross-section) the resulting optimal configuration has a tenfold increase in surface interfacial area compared to a fully circular cross section. As well, when the substrate does not like the polymer (nonwet case) there is a large energy penalty for forming substrate-polymer contact area, resulting in a much larger force to compress the chain. In the stretching case, only a small force was required because, after a small anisotropic deformation, the chain unraveled to a tadpole. In the compression case this is not possible.

CONCLUSION

In this paper, we have examined some scenarios where toroids of semiflexible polymers are deformed. We have adopted the simplest possible model of toroids where the chains are densely packed and where the radius is determined by a balance between chain bending (which favors large radii) and surface energy (which favors small radii). Some physics is certainly absent from this model. For instance, the effect of shape fluctuations is totally ignored. We neglect electrostatic interactions and van Der Waals forces, which can be important for DNA in some regimes. For example, the presence of van der Waals forces are known to change the order and position of the wetting transition in binary polymer fluids (Schmidt and Binder, 1985). We have also assumed that the density of the toroid is constant throughout the volume, thereby neglecting excluded volume effects. To account for such effects, one would need to introduce virial terms. However such treatments are beyond the scope of the present paper. The basic reason for not discussing these complicating effects is one of simplicity. Because this is the first study of DNA adsorption, stretching, and compression, we feel the basic physics has been included, and including further effects would severely complicate the physics (and mathematical analysis). The most important case experimentally concerns the adsorption to surfaces, where an increase in radius occurs upon adsorption. One main conclusion from this simple model is that, if a toroid exists in the bulk, it should also exist when adsorbed to a surface and vice-versa.

We have also studied two other kinds of simple deformation: stretching and compression. When stretched at fixed displacement, the toroid undergoes a transition from an ellipse to a tadpole regime. In the elliptical regime the force varies linearly with stretching distance, whereas in the tadpole regime the force is constant. Under compression, the form of the force law depends on how strongly the polymer wets the surfaces. For strongly nonwetting conditions, i.e., $\theta = \pi$, the force varies inversely as the cube of the compressional distance, whereas for $\pi/2 < \theta < \pi$, the force varies inversely as the square of the compressional distance. In both these cases a (positive) force is required to compress the chain. When $\theta \leq \pi/2$, a force, inversely proportional to the square of the separation, is required to keep the plates from collapsing together. The main reason for this is that the polymer wants to spread over the surfaces, which implies a preferred minimal separation of the plates.

The authors acknowledge support from an Australian Research Council Large Grant. D. R. M. W. is supported by an Australian Research Council Queen Elizabeth II.

REFERENCES

Abramowitz, M., and I. Stegun. 1970. Handbook of Mathematical Functions, Dover Publications, New York. 587–627.

Argaman, M., R. Golan, N. H. Thomson, and H. G. Hansma. 1997. Phase imaging of moving DNA molecules replicated in the atomic force microscope. *Nucleic Acids Res.* 25:4379–4384.

Bloomfield, V. A. 1997. DNA condensation by multivalent ions. *Biopolymers.* 44:269–282.

Bloomfield, V. A. 1991. Condensation of DNA by multivalent cations; considerations on mechanism. *Biopolymers.* 31:1471–1481.

Bright, J. N., and D. R. M. Williams. 1999. Grafted semiflexible polymers in poor solvents: toroidal and tower surfaces micelles. *Europhys. Lett.* 45:321–326.

Duguid, J. G., C. Li, M. Shi, M. J. Logan, H. Alila, A. Rolland, E. Tomlinson, J. Sparrow, and L. C. Smith. 1998. A physiochemical approach for predicting the effectiveness of peptide-based gene delivery systems for use in plasmid based gene therapy. *Biophys. J.* 74: 2802–2814.

Fang, Y., T. S. Spisz, and J. H. Hoh. 1999. Ethanol-induced structural transitions of DNA on mica. *Nucleic Acids Res.* 27:1943–1949.

Fang, Y., and J. H. Hoh. 1998. Early intermediates in spermidine-induced DNA condensation on the surface of mica. *J. Am. Chem. Soc.* 120: 8903–8909.

Feng, Y., and J. H. Hoh. 1998. Surface-directed DNA condensation in the absence of soluble multivalent cations. *Nucleic Acids Res.* 26:588–593.

Golan, R., L. I. Pietrasanta, W. Hseih, and H. G. Hansma. 1999. DNA toroids: stages in condensation. *Biochemistry.* 38:14069–14076.

Guthold, M., X. S. Zhu, C. Rivetti, G. L. Yang, N. H. Thompson, S. Kasas, H. G. Hansma, B. Smith, P. K. Hansma, and C. Bustmante. 1999. Direct observation of one-dimensional diffusion and transcription by *Escherichia coli* RNA polymerase. *Biophys. J.* 77:2284–2294.

Grosberg, A. Y. 1979. Certain possible conformational states of a uniform elastic polymer chain. *Biophysics.* 24:30–36.

Halperin, A., and E. B. Zhulina. 1991. On the deformation behavior of collapsed polymers. *Europhys. Lett.* 15:417–421.

Hansma, H. G., R. Golan, W. Hsieh, C. P. Lollo, P. Mullenley, D. Kwoh. 1998. DNA Condensation for gene therapy as monitored by atomic force microscopy. *Nucleic Acids Research.* 26:2481–2487.

Hansma, H. G., and L. Pietrasanta. 1998. Atomic force microscopy and other scanning probe microscopies. *Curr. Opin. Chem. Biol.* 2:579–584.

Hansma, H. G. 1999. Varieties of imaging with scanning probe microscopes. *Proc. Natl. Acad. Sci. USA.* 96:14678–14680.

Hansma, H. G., and D. E. Laney. 1996. DNA binding to mica correlates with cationic radius—assay by atomic force microscopy. *Biophys. J.* 70:1933–1939.

Hansma, H. G., D. E. Laney, M. Bezanilla, R. L. Sinhsheimer, and P. K. Hansma. 1995. Applications for atomic force microscopy of DNA. *Biophys. J.* 68:1672–1677.

Hud, N. V., K. H. Downing, and R. Balhorn. 1995. A constant radius of curvature model for the organization of DNA in toroidal condensates. *Proc. Natl. Acad. Sci. USA.* 92:3581–3585.

Marshall, E. 1995. Gene therapy's growing pains. *Science.* 269: 1050–1055.

Odijk, T. 1996. DNA in a liquid–crystalline environment: Tight bends, rings, and supercoils. *J. Chem. Phys.* 105:1270–1286.

Park, S. Y., D. Harries, and W. M. Gelbart. 1998. Topological defects and the optimum size of DNA condensates. *Biophys. J.* 75:714–720.

Perales, J. C., T. Ferkol, M. Molas, and R. W. Hanson. 1994. An evaluation of receptor-mediated gene-transfer using synthetic DNA-ligand complexes. *Eur. J. Biochem.* 226:255–266.

Phillips, S. C. 1995. Receptor-mediated DNA delivery approaches to human gene therapy. *Biologicals.* 23:13–16.

Plateau, J. A. F. 1873. Statique experimentale et Theorique des Liquides soumis aux seules Forces moleculaires. Gauthier-Villars, Paris. 71–98.

Radmacher, M., J. P. Cleveland, M. Fritz, H. G. Hansma, and P. K. Hansma. 1994. Mapping interaction forces with the atomic force microscope. *Biophys. J.* 66:2159–2165.

Rayleigh, (Lord) J. W. S. 1879. On the instability of jets. *Proc. London Math. Soc.* 10:4–13.

Schmidt, I., and K. Binder. 1985. Model calculations for wetting transitions in polymer mixtures. *J. Phys. (Paris).* 46:1631–1639.

Ubbink, J., and T. Odijk. 1995. Polymer- and salt-induced toroids of hexagonal DNA. *Biophys. J.* 68:54–61.

Vasilevskaya, V. V., A. R. Khokhlov, S. Kidoaki, and K. Yoshikawa. 1997. Structure of collapsed persistent macromolecule—toroid versus spherical globule. *Biopolymers.* 41:51–60.

Yoshikawa, Y., K. Yoshikawa, and T. Kanbe. 1996. Daunomycin unfolds compactly packed DNA. *Biophys. Chem.* 61:93–100.